

VU Research Portal

Why is the force-velocity relationship in leg press tasks quasi-linear rather than hyperbolic?

Bobbert, M.F.

published in

Journal of Applied Physiology (1985)
2012

DOI (link to publisher)

[10.1152/jappphysiol.00787.2011](https://doi.org/10.1152/jappphysiol.00787.2011)

document version

Publisher's PDF, also known as Version of record

[Link to publication in VU Research Portal](#)

citation for published version (APA)

Bobbert, M. F. (2012). Why is the force-velocity relationship in leg press tasks quasi-linear rather than hyperbolic? *Journal of Applied Physiology* (1985), 112, 1975-1983.
<https://doi.org/10.1152/jappphysiol.00787.2011>

General rights

Copyright and moral rights for the publications made accessible in the public portal are retained by the authors and/or other copyright owners and it is a condition of accessing publications that users recognise and abide by the legal requirements associated with these rights.

- Users may download and print one copy of any publication from the public portal for the purpose of private study or research.
- You may not further distribute the material or use it for any profit-making activity or commercial gain
- You may freely distribute the URL identifying the publication in the public portal ?

Take down policy

If you believe that this document breaches copyright please contact us providing details, and we will remove access to the work immediately and investigate your claim.

E-mail address:

vuresearchportal.ub@vu.nl

Why is the force-velocity relationship in leg press tasks quasi-linear rather than hyperbolic?

Maarten F. Bobbert

J Appl Physiol 112:1975-1983, 2012. First published 22 March 2012;
doi:10.1152/jappphysiol.00787.2011

You might find this additional info useful...

This article cites 35 articles, 9 of which can be accessed free at:

<http://jap.physiology.org/content/112/12/1975.full.html#ref-list-1>

Updated information and services including high resolution figures, can be found at:

<http://jap.physiology.org/content/112/12/1975.full.html>

Additional material and information about *Journal of Applied Physiology* can be found at:

<http://www.the-aps.org/publications/jappl>

This information is current as of June 16, 2012.

Why is the force-velocity relationship in leg press tasks quasi-linear rather than hyperbolic?

Maarten F. Bobbert

Research Institute MOVE, Faculty of Human Movement Sciences, VU University Amsterdam, Amsterdam, The Netherlands

Submitted 27 June 2011; accepted in final form 17 March 2012

Bobbert MF. Why is the force-velocity relationship in leg press tasks quasi-linear rather than hyperbolic? *J Appl Physiol* 112: 1975–1983, 2012. First published March 22, 2012; doi:10.1152/jappphysiol.00787.2011.—Force-velocity relationships reported in the literature for functional tasks involving a combination of joint rotations tend to be quasi-linear. The purpose of this study was to explain why they are not hyperbolic, like Hill's relationship. For this purpose, a leg press task was simulated with a musculoskeletal model of the human leg, which had stimulation of knee extensor muscles as only independent input. In the task the ankles moved linearly, away from the hips, against an imposed external force that was reduced over contractions from 95 to 5% of the maximum isometric value. Contractions started at 70% of leg length, and force and velocity values were extracted when 80% of leg length was reached. It was shown that the relationship between leg extension velocity and external force was quasi-linear, while the relationship between leg extension velocity and muscle force was hyperbolic. The discrepancy was explained by the fact that segmental dynamics canceled more and more of the muscle force as the external force was further reduced and velocity became higher. External power output peaked when the imposed external force was ~50% of maximum, while muscle power output peaked when the imposed force was only ~15% of maximum; in the latter case ~70% of muscle power was buffered by the leg segments. According to the results of this study, there is no need to appeal to neural mechanisms to explain why, in leg press tasks, the force-velocity relationship is quasi-linear rather than hyperbolic.

muscle power; multijoint leg extension; dynamometer; forward dynamics

THE MAXIMAL STEADY-STATE FORCE that a muscle can produce diminishes as the velocity of shortening is increased. In 1935, Fenn and Marsh (10) were the first to investigate the force-velocity relationship in isotonic shortening experiments on isolated frog and cat muscles and showed it to be exponential. Three years later, Hill (13) performed thermodynamic experiments on shortening frog muscle and derived the well-known hyperbolic equation relating force F to velocity V :

$$(F + a) \cdot (V + b) = \text{constant} = (F_0 + a) \cdot b \quad (1)$$

where a and b are positive constants and F_0 is isometric force. In 1957, Hill's phenomenological relationship received a structural underpinning when Huxley (15) formulated the cross-bridge model and showed that its predictions could be made to fit Eq. 1.

Address for reprint requests and other correspondence: M. F. Bobbert, Research Institute MOVE, Faculty of Human Movement Sciences, VU Univ. Amsterdam, Van der Boerhorstraat 9, 1081 BT Amsterdam, The Netherlands (e-mail: M_F_Bobbert@fbw.vu.nl).

Provided that the rate of change of series elastic element (SEE) length is small or accounted for, Hill's rectangular hyperbola describes with remarkable accuracy combinations of force and velocity obtained in numerous experiments with different types of apparatus on isolated and artificially stimulated muscles of animals (for references, see Ref. 1), isolated and voluntarily activated human muscle (e.g., Ref. 21), as well as combinations of force and velocity obtained in voluntary maximal isotonic elbow flexions (34). Relationships between joint moment and angular velocity in maximum voluntary isokinetic extensions of individual joints also generally adhere to Hill's rectangular hyperbola (for references, see Ref. 4), albeit that in some studies deviations have been reported at low angular velocities, which were attributed to neural inhibition (19, 33).

Force-velocity relationships have been studied not only in single-joint rotations, but also in more functional tasks that involve a combination of joint rotations. Interestingly, the relationships obtained in these tasks are quasi-linear rather than hyperbolic like Hill's relationship. Linear relationships have been described for hand-rim propulsion force as a function of rim speed in wheelchair sprinting (14), peak pedal force as a function of crank velocity in sprint cycling (2, 24, 31), instantaneous torque as a function of velocity at peak power in cycling against a range of inertial loads (18), average force as a function of average velocity in half-squat exercises performed with a range of added masses (7, 20), force and velocity in leg press against a dynamometer in "isotonic mode" (17), peak force as a function of peak velocity in explosive leg extension against a range of added isotonic forces on a sledge dynamometer (22), and force and velocity in combined knee and hip extension on a servo-controlled dynamometer (35–37). Especially the results of Yamauchi et al. (35–37) are puzzling in this respect, because the investigators made an admirable attempt to mimic as closely as possible the isotonic conditions used in the classical experiments on isolated animal muscle (10, 13). To explain why the force-velocity relationship in these more functional tasks was quasi-linear rather than hyperbolic, it has been proposed that multijoint tasks are challenging from a coordinative point of view and that "... some neural mechanisms may be involved in the force-velocity relation of the knee-hip extension movement ...", which "... make it exhibit a linear appearance rather than a hyperbola" (35).

Before appealing to neural mechanisms to explain why force-velocity relationships in functional tasks are quasi-linear rather than hyperbolic, I propose to investigate whether the explanation can perhaps be found in segmental dynamics. After all, linear motion of an end-effector, such as the foot, involves rotations of body segments, and the

angular velocities and angular accelerations of the segments affect the contact force between the end-effector and the environment (5, 6, 26).

In the present study, I used a forward simulation model to determine to what extent the force-velocity relationship is affected by segmental dynamics in the hip-knee extension task of Yamauchi et al. (35), henceforth referred to as “leg press task.” I also studied the effect on the power-velocity relationship, because it has been suggested that the loading conditions leading to peak power should be selected as the conditions to be used in training programs for power production (37).

MATERIALS AND METHODS

For the simulations, I used the two-dimensional forward dynamic model of the human musculoskeletal system schematically shown in Fig. 1. The model, which had muscle stimulation (STIM) over time as its only independent input, consisted of four rigid segments: one HAT segment, representing head, arms, and trunk; one segment representing the thighs; one segment representing the shanks; and one segment representing the feet. These segments were interconnected by hinges representing hip, knee, and ankle joints. The rotational degree of freedom of the feet was fixed, to mimic that the feet were strapped to a sliding foot plate, and the rotational and translational degrees of freedom of the HAT segment were fixed to mimic that the subject's trunk was strapped to a nonmovable chair. As a result, the model as a whole had only one degree of freedom: given the lengths of the segments, the kinematic constraints and the known position of the hips in space, only one coordinate (for example the position of the ankles, or the hip angle) was needed to fully determine all other coordinates of the system. Segmental parameters were the same as those used in a model for simulation of two-leg jumping, which was previously described in full detail (30).

Within the skeletal submodel, only the muscle-tendon complex of *mm. vasti* was embedded, causing the model to be a simplified version of the original model additionally comprising the muscle-tendon complexes of *m. gluteus maximus*, hamstrings, *m. rectus femoris*, *m. soleus*, and *m. gastrocnemius* (30). My motivation to do so is provided in APPENDIX A. Briefly, all of the muscle-tendon

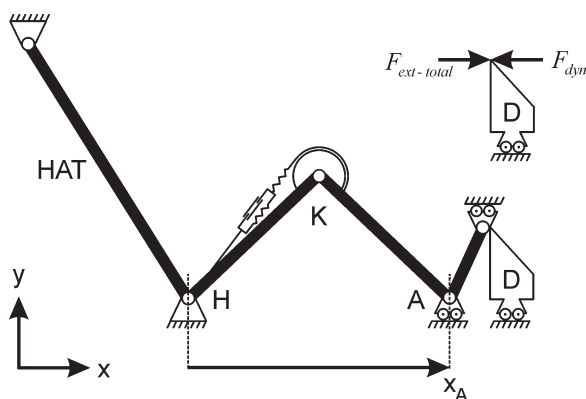


Fig. 1. Model used for simulation of the leg press task. The head-arms-trunk (HAT) segment was fixed in space, the ankles (A) could only move horizontally, and the angle of the feet was fixed. Rightward movement of A caused extension in the hip joints (H), extension in the knee joints (K), and plantar flexion. The total horizontal force produced on the environment along the x -axis ($F_{\text{ext-total}}$) was counteracted by the force of a dynamometer D (F_{dyn}). The system was actuated by *mm. vasti* (VAS), modeled as a Hill-type unit. The only input of the model was muscle stimulation as a function of time. The distance between A and H is referred to as x_A .

complexes (see Fig. A1) shorten monotonically during the leg press task simulated in this study. It follows that each of them individually produces a positive (rightward directed) force on the dynamometer during the leg press task. Hence, the outcome of the simulations will be qualitatively the same, regardless of which individual muscle-tendon complex, or combination of muscle-tendon complexes, is selected to actuate the system. The advantage of using only one muscle-tendon complex as actuator was that the results could be presented in a concise manner, and selecting the muscle-tendon complex of *mm. vasti* was a logical choice because it has the largest contribution to the force exerted on the dynamometer (see APPENDIX A).

The model of the muscle-tendon complex, which has also been described in full detail elsewhere (28), consisted of a contractile element (CE), an SEE, and a parallel elastic element (PEE). Briefly, behavior of SEE and PEE was determined by a quadratic force-length relationship, while behavior of CE was more complex: CE velocity depended on CE length, force, and active state, with the latter being defined as the relative amount of calcium bound to troponin (9). The dependence of shortening velocity on force was modeled using Hill's hyperbola, with F_0 depending on CE length and active state. Following Hatze (12), the relationship between active state and STIM was modeled as a first-order process. STIM, ranging between 0 and 1, was a one-dimensional representation of the effects of recruitment and firing frequency of α -motoneurons. A change toward 1 occurred at a rate of 5/s, a value previously used to match simulated and experimental ground reaction force curves in maximum height squat jumping (3). The maximum F_0 at optimum length of *mm. vasti* in the model was 9,000 N (i.e., 4,500 N per leg), and the constant moment arm at the knee joint was 4.2 cm. Other relevant parameters were $l_{\text{CE,opt}} = 9.3$ cm (optimum CE length), $b = 5.2 l_{\text{CE,opt}}/\text{s}$, and $a/F_0 = 0.41$. The complete set of parameter values can be found elsewhere (28).

I used the model to simulate isometric and dynamic contractions with STIM(t) as the only input. The isometric contractions were performed at configurations corresponding to various distances between ankles and hips (x_A). These distances will be expressed as percentages of the maximum distance, henceforth referred to as “leg length” (LL). The starting configuration used for the dynamic contractions corresponded to 70%LL (35). The ankles (A) remained fixed in the initial position until the force at the feet generated by *mm. vasti* was equal in magnitude but opposite to the imposed force and were subsequently released. After release, the imposed force varied as a function of position in such a way that, in each configuration, it was a constant fraction of the F_0 at that configuration (35). Given the initial state and STIM as a function of time (i.e., ramped at 5/s), the resulting movement was calculated through numerical integration using a variable order, variable step size, Adams-Bashford predictor, and Adams-Moulton corrector algorithm (25). Once the movement had been found, I determined the separate contributions to the total external force ($F_{\text{ext-total}}$) of 1) the knee joint moment (M_K) generated by *mm. vasti* ($F_{\text{ext-vasti}}$), 2) gravity ($F_{\text{ext-gravity}}$), 3) the angular accelerations of the segments, and 4) the angular velocities of the segments. The method used to determine these contributions is detailed in APPENDIX B.

Because I was not interested in the latter two contributions separately, I will only present the total (mostly negative) contribution of segmental dynamics ($F_{\text{ext-SD}}$). This contribution may be thought of as the force that one experiences when grabbing both ankles and moving them away from the hips in the absence of knee extension moments and gravity.

RESULTS

Figure 2, left, shows how, in isometric contractions (fraction $f = 1$) at maximum STIM, the M_K , $F_{\text{ext-total}}$, $F_{\text{ext-vasti}}$, and $F_{\text{ext-gravity}}$ vary with x_A . Because of the geometric

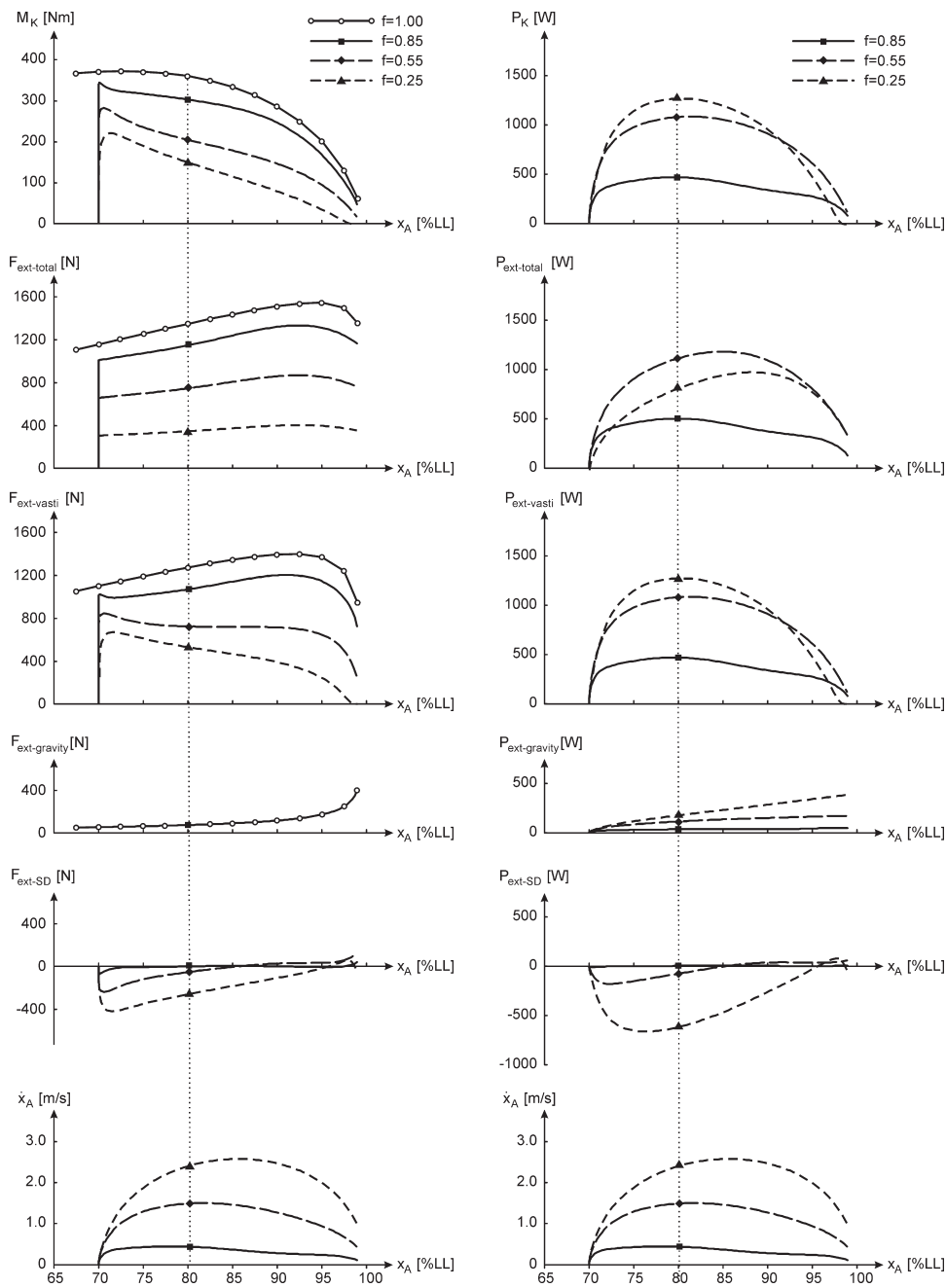


Fig. 2. Simulation results obtained at different fractions (f) of imposed force F_{dyn} , plotted over x_A , expressed in percentages of leg length (%LL). At $f = 1$, the contractions are isometric: the imposed F at a given x_A is equal but opposite to the $F_{\text{ext-total}}$ (see Fig. 1) in a maximum isometric contraction at that x_A . At smaller values for f , leg extension occurred: at each x_A reached during leg extension, the F_{dyn} was f times the F_{dyn} in the maximum isometric contraction at that x_A . *Left from the top to bottom:* knee extension moment (M_K), $F_{\text{ext-total}}$ (see Fig. 1), contribution to $F_{\text{ext-total}}$ by muscle ($F_{\text{ext-vasti}}$), contribution to $F_{\text{ext-total}}$ by gravity ($F_{\text{ext-gravity}}$), contribution to $F_{\text{ext-total}}$ by segmental dynamics ($F_{\text{ext-SD}}$), and velocity (i.e., rate of change x_A). *Right:* power (P) of M_K at each of the F values mentioned ($P_{\text{ext-total}}$, $P_{\text{ext-vasti}}$, $P_{\text{ext-gravity}}$, $P_{\text{ext-SD}}$). Dashed vertical line at $x_A = 80\%$ indicates where instantaneous values were extracted from each of the curves for construction of Fig. 3.

transfer function, $F_{\text{ext-vasti}}$ and $F_{\text{ext-total}}$ peak at a larger x_A than M_K . Also because of the geometric transfer function, $F_{\text{ext-gravity}}$ increases when the leg becomes more extended.

For the dynamic contractions at imposed submaximal forces, I made the imposed force dependent on x_A by fitting a polynomial function to $F_{\text{ext-total}}$ over x_A in the isometric contractions and scaling this function by a fraction f (note that the imposed force is always equal in magnitude but opposite in direction to $F_{\text{ext-total}}$, see Fig. 1). This approach was adopted from Yamauchi et al. (35), who used it in an attempt to make the muscle contract at a constant f of its length-dependent F_0 throughout the motion (note that this is not perfectly correct, if only because $F_{\text{ext-gravity}}$ depends on x_A as well and because it is possible that, in a human subject, the relative contributions of

different muscles to the force on the dynamometer change throughout the movement). Fig. 2 also shows the results of dynamic contractions at $f = 0.85$, $f = 0.55$, and $f = 0.25$. During the dynamic contraction at $f = 0.85$, $F_{\text{ext-vasti}}$ as a function of x_A is more or less a constant fraction of the isometric $F_{\text{ext-vasti}}$ as a function of x_A . At $f = 0.25$, however, this is not the case. At $f = 0.25$, M_K increases over the first part of the range of motion because active state still increases after the start of movement. More importantly, the tight relationship between $F_{\text{ext-vasti}}$ and $F_{\text{ext-total}}$ that existed in the isometric contractions is lost, because $F_{\text{ext-SD}}$ substantially interferes. $F_{\text{ext-SD}}$ is negative and becomes more negative as f is further reduced, causing the discrepancy between $F_{\text{ext-vasti}}$ and $F_{\text{ext-total}}$ to become larger.

Figure 2, *right*, shows power output (P_K) obtained by multiplying M_K by knee angular velocity, as well as the power outputs of the different contributions to the $F_{\text{ext-total}}$ obtained by multiplying the forces by \dot{x}_A (see *bottom*). Obviously, P_K equals the power output of the muscle, and also equals power $P_{\text{ext-vasti}}$. As f is further reduced, more and more of the muscle's power output is buffered by the segments (negative $P_{\text{ext-SD}}$) and does not contribute to $P_{\text{ext-total}}$.

Yamauchi et al. (35) constructed their force-velocity relationships by plotting combinations of \dot{x}_A and $F_{\text{ext-total}}$, reached at the point of passing 80%LL (vertical dashed lines in Fig. 2) at different values for f . If I do the same for my simulated contractions, Fig. 3 is obtained. The overall force-velocity relationship, i.e., the relationship between $F_{\text{ext-total}}$ and \dot{x}_A , is indeed quasi-linear. However, the relationship between $F_{\text{ext-vasti}}$ and \dot{x}_A , which is obviously the true relationship of interest, still has the shape of a rectangular hyperbola. Note that slight deviations from Hill's curve may occur because 1) at low imposed forces, the active state may not yet have reached its maximum at 80%LL, and 2) dif-

ferent force levels imply different SEE extensions and hence different CE lengths. When we compare the relationship between $F_{\text{ext-total}}$ and \dot{x}_A to the relationship between $F_{\text{ext-vasti}}$ and \dot{x}_A , the main point becomes clear: segmental dynamics are at least one important reason why the force-velocity relationship in more functional tasks is quasi-linear and not hyperbolic.

It is tempting to extrapolate linear relationships, for instance to find F_0 (the force produced isometrically) and v_0 , i.e., the value of \dot{x}_A , where $F_{\text{ext-total}}$ is zero (22, 23, 35). F_0 is not too interesting because it can directly be measured. Is v_0 interesting and meaningful? In Fig. 3, v_0 is calculated to be 3.2 m/s. Clearly, this value has nothing to do with the speed \dot{x}_A at which the shortening velocity of CE is maximal; starting from the maximal shortening velocity of the muscle fibers, the corresponding \dot{x}_A is calculated to be close to 10 m/s. Furthermore, and unfortunately, v_0 depends on the specific conditions under which the experiments are conducted. In Fig. 3, which was constructed using combinations of \dot{x}_A and $F_{\text{ext-total}}$ extracted at 80%LL, v_0 was found to be 3.2 m/s, but, with combinations

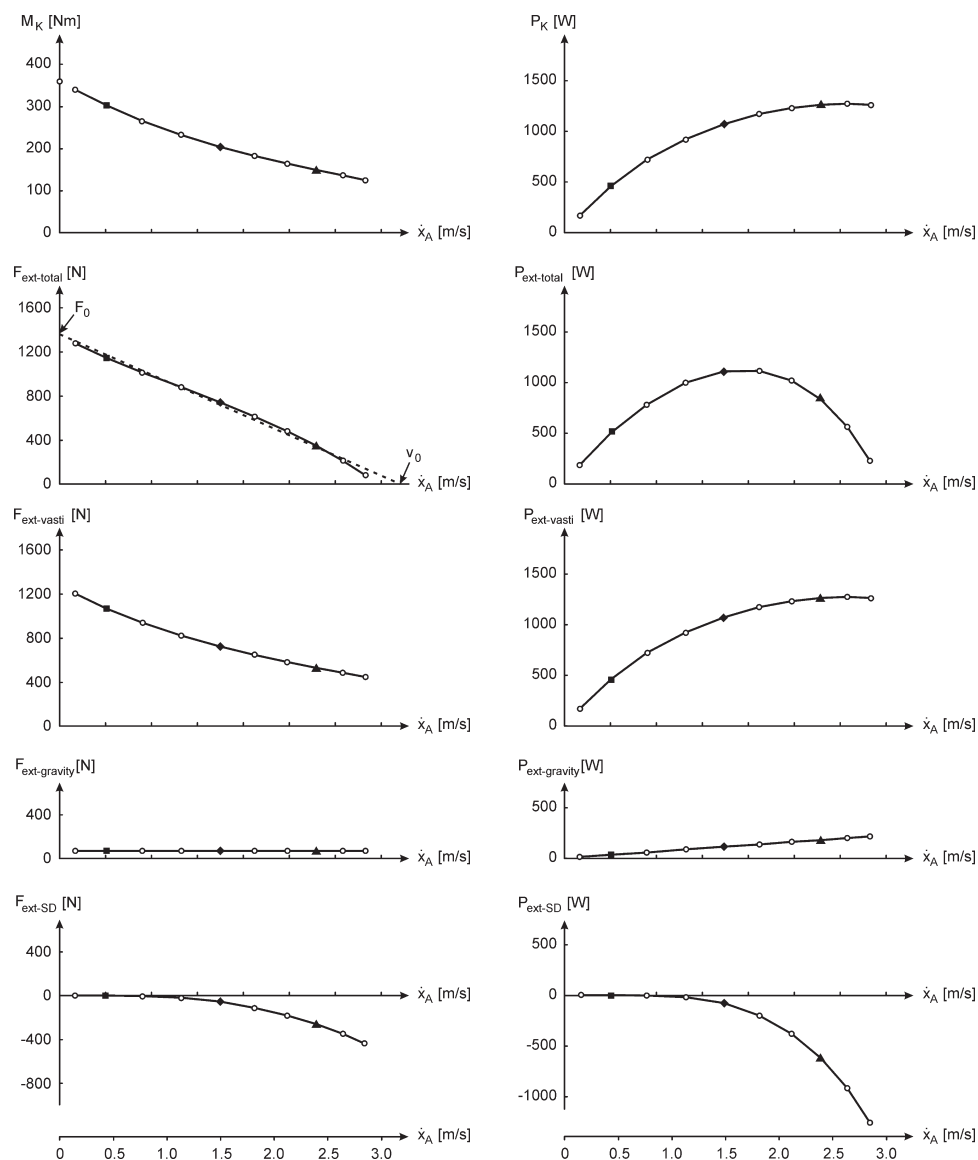


Fig. 3. Knee extension moment (M_K), force (F), and power (P) as a function of velocity of A relative to H (\dot{x}_A), extracted at $x_A = 80\%$ LL from simulated contractions, as shown in Fig. 2 (note corresponding symbols) and simulated contractions at other f of imposed F (f was lowered from 0.95 to 0.05 in steps of 0.1). Variables for F and P correspond to those in Fig. 2. A line fitted to combinations of $F_{\text{ext-total}}$ and \dot{x}_A (left, second panel) intersects the F axis at the point $(0, F_0)$ and the velocity axis at $(v_0, 0)$.

extracted at 77%LL, v_0 was 2.8 m/s, and with combinations extracted at 85%LL v_0 was 3.5 m/s (results not shown). Samozino et al. (23) extrapolated a line fitted to combinations of average force (force averaged over displacement) and average velocity (\dot{x}_A averaged over displacement). Taking this same approach with the model, I found a v_0 of 2.55 m/s when the contractions were initiated from 70%LL, and a v_0 of 2.88 m/s when the contractions were initiated from 60%LL (comparison of my absolute values for v_0 with those of Samozino et al. is not useful because my model incorporated only *mm. vasti*).

Finally, it needs no further argument that the relationship between external power $P_{\text{ext-total}}$ and \dot{x}_A , determined by imposing different loads and measuring power output at the same x_A , is completely different from the relationship between muscle power $P_{\text{ext-vasti}}$ and \dot{x}_A (Fig. 3, right). $P_{\text{ext-total}}$ peaks about midway between $\dot{x}_A = 0$ and $\dot{x}_A = v_0$, as was reported by Yamauchi et al. (35), but $P_{\text{ext-vasti}}$ peaks close to v_0 . The latter is again not surprising, because, at v_0 , the muscle fibers are shortening at $\sim 30\%$ of their maximum shortening velocity, close to the velocity at which they can indeed produce maximum power.

DISCUSSION

The purpose of this paper was to explain why force-velocity relationships reported in the literature for functional tasks involving a combination of joint rotations tend to be quasi-linear, rather than hyperbolic like Hill's relationship. For this purpose, I simulated a hip-knee extension task of Yamauchi et al. (35) with a musculoskeletal model. I showed that, for this particular leg press task, the relationship between leg extension and external force is quasi-linear, while the relationship between leg extension velocity and muscle force is hyperbolic (Fig. 3, left). This discrepancy is explained by the fact that segmental dynamics cancel more and more of the muscle force as the velocity becomes larger. Thus there is no need to appeal to neural mechanisms to explain why in this task the force-velocity relationship is quasi-linear rather than hyperbolic like Hill's relationship.

It may be argued that the model contained only the monoarticular *mm. vasti* and, therefore, was too simple to study a motor task that requires coordination among multiple muscles acting about different joints in the leg. However, I feel that this is actually one of the strengths of the model: even a simple model with only one maximally stimulated muscle reproduced the phenomenon to be explained. Still, it may well be that neural mechanisms also come into play in reality, as suggested by Yamauchi et al. (35). Let me elaborate on this possibility from a mechanical perspective. In order for neural mechanisms to explain why, in this task, the force-velocity relationship is quasi-linear rather than hyperbolic, it must be so that muscle activation varies among contractions at different imposed forces and hence velocities. This could occur if muscles had to vary their stimulation, depending on the configuration of the leg. For example, if a muscle were to change from shortening to lengthening beyond a particular value of x_A , it would have to be deactivated to prevent it from reducing the mechanical output. As movement speed goes up over contractions, deactivation would have to occur at a smaller x_A , because

active state dynamics are relatively slow. However, the leg press task is a one degree of freedom task, in which the monoarticular muscle-tendon complexes (*m. gluteus maximus*, *mm. vasti*, and *m. soleus*), as well as the biarticular muscle-tendon complexes (hamstrings, *m. rectus femoris*, and *m. gastrocnemius*) all shorten monotonically (APPENDIX A, see Fig. A2). Each of these individual muscle-tendon complexes produces the highest mechanical output on the dynamometer when it is simply maximally activated over the full range of motion. Hence, from the perspective of maximizing the mechanical output during the leg press task, there is no reason why muscle activation should vary among contractions and thereby cause the force-velocity relationship to be quasi-linear rather than hyperbolic. Needless to say, however, this mechanical analysis does not rule out the possibility that, in reality, neural mechanisms do contribute, as suggested by Yamauchi et al. (35).

Can the findings of this paper be generalized to other tasks in which quasi-linear force-velocity relationships have been found? Let us begin by noting that, in leg press tasks like the one studied in this paper, segmental dynamics will tend to play a similar role, regardless of whether the combinations of velocity and force were obtained in velocity-controlled contractions (e.g., at constant \dot{x}_A ; Ref. 16), in force-controlled contractions, or in ballistic contractions; at a given combination of x_A and \dot{x}_A , the segmental dynamics are the same, regardless of how this combination was reached. Hence, segmental dynamics will also explain, at least partly, why quasi-linear force-velocity relationships have been found in half-squat exercises performed with a range of added masses (7, 20), force and velocity in leg press against a dynamometer in "isotonic mode" (17), and peak force as a function of peak velocity in explosive leg extension against a range of added isotonic forces on a sledge dynamometer (22). The same will hold for hand-rim propulsion force in wheelchair sprinting (14), essentially an arm press task comparable to the leg press tasks mentioned above.

Linear relationships have also been described for peak pedal force as a function of crank velocity in sprint cycling (2, 24, 31) and for instantaneous torque as a function of velocity at

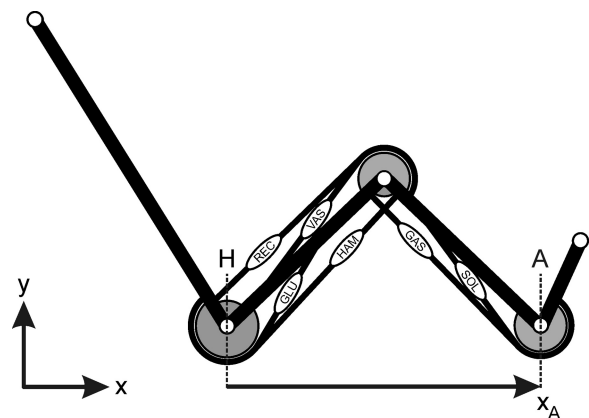


Fig. A1. Original musculoskeletal model (30) containing not only VAS but also *m. gluteus maximus* (GLU), hamstrings (HAM), *m. rectus femoris* (REC), *m. soleus* (SOL), and *m. gastrocnemius* (GAS). Note that, because of space limitations in the figure, the moment arms of the muscle-tendon complexes at the joints (gray spacers at the joints) have not been drawn to scale.

peak power in cycling against a range of inertial loads (18). In cycling, segmental dynamics will play a similar role as in leg press tasks, but there is another factor that contributes: the relative slowness of active state dynamics. Maximization of average power output of a muscle in cycling requires the active state to be as high as possible in the phase where the muscle shortens (to maximize work production) and as low as possible in the phase where it lengthens (to minimize energy dissipation). Because of its relative slowness, active state will not be maximal over the full shortening phase and will not be zero during the full lengthening phase at high pedaling rates (29). Consequently, as pedaling rate goes up, pedal force during the down stroke will be reduced, both because of the increase in shortening velocity of leg extensors and because of a decrease in their active state. In trying to understand why in cycling the force-velocity relationship is quasi-linear rather than hyperbolic, we should, therefore, take into account not only segmental dynamics but also variations in active state.

What are the implications of the findings of this study for the selection of training loads? From a physiological point of view,

training loads should be selected on the basis of muscle mechanical output (force and/or power) and not on the basis of external mechanical output. From Fig. 3, it will be obvious that the relationship between muscle mechanical output and velocity is very different from the relationship between external mechanical output and velocity. Note that external power peaks at intermediate loads (f close to 0.5), while muscle power peaks at the lowest loads (f close to 0.15). To derive the relationship between muscle mechanical output and velocity, the best one can do is determine the net mechanical output about the joints by combining measured kinematics and contact forces in an inverse dynamics analysis (27).

What are the implications of the findings of this study for models that build on the quasi-linear relationship between external force and velocity as measured in functional tasks? In a recent study, Samozino et al. (23) outlined a theoretical approach to better understand the mechanical factors affecting jumping performance. In that approach, two mechanical characteristics of the leg force generator play a role: the maximal force that can be produced (F_0) and the maximal velocity at

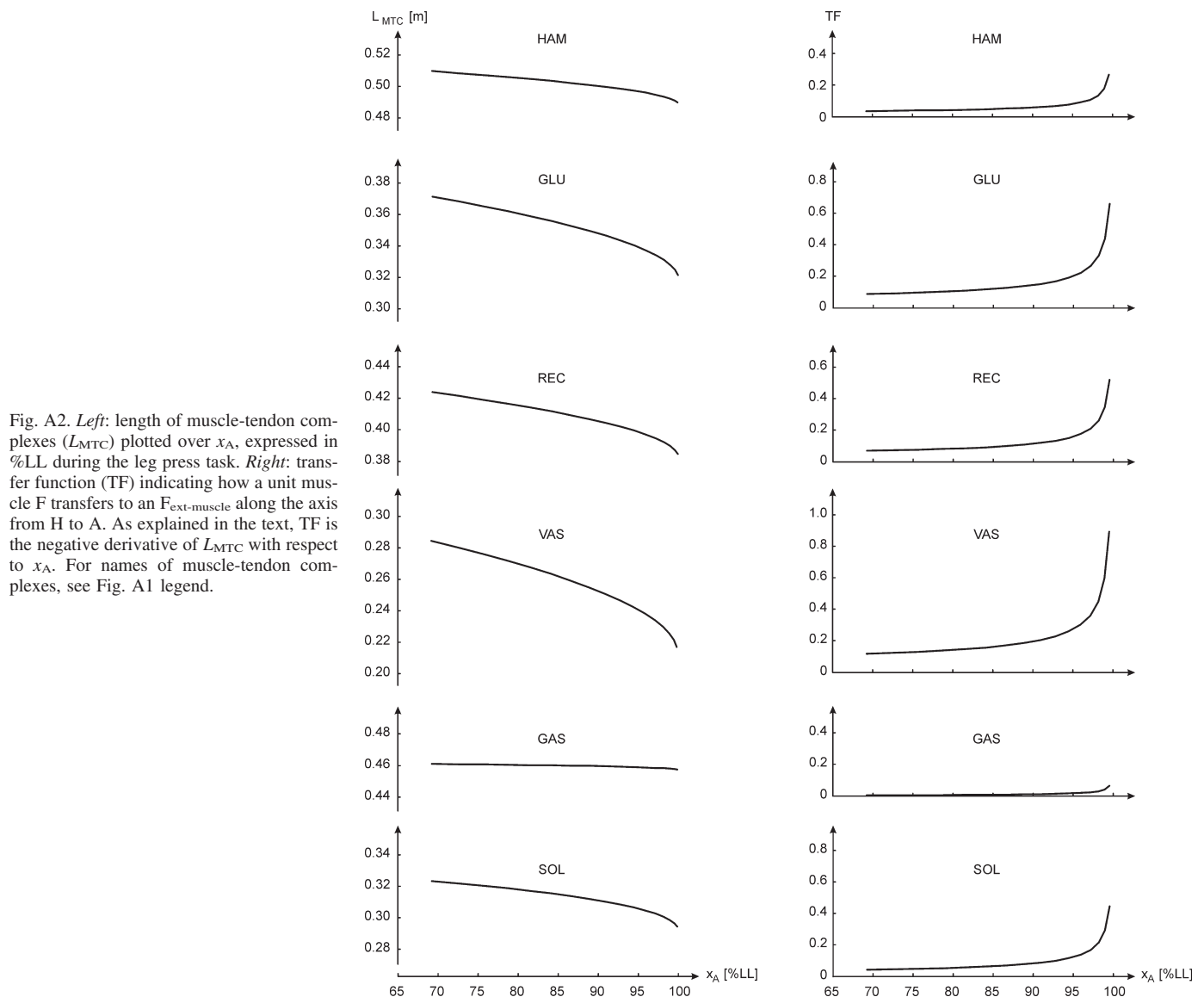


Fig. A2. *Left:* length of muscle-tendon complexes (L_{MTC}) plotted over x_A , expressed in %LL during the leg press task. *Right:* transfer function (TF) indicating how a unit muscle F transfers to an $F_{ext-muscle}$ along the axis from H to A. As explained in the text, TF is the negative derivative of L_{MTC} with respect to x_A . For names of muscle-tendon complexes, see Fig. A1 legend.

which the leg can be extended by muscle action (v_0). Both characteristics are obtained by extrapolation of a relationship between external force and velocity like the one shown in Fig. 3. The authors attributed the mechanical characteristics of the leg force generator mainly to the mechanical properties of muscles. From the results of the present paper, however, it will be clear that the mechanical characteristics of the leg force generator are strongly influenced by segmental dynamics. Hence, as mentioned in the results section, the extrapolated F_0 and v_0 depend on the precise conditions under which combinations of external force and leg extension velocity are obtained. The approach of Samozino et al. (23) is not only limited in the sense that it builds on phenomenological relationships that first need to be determined experimentally; it also ignores that predictions of jumping performance can only be made, and insight into jumping mechanics only gained, if segmental dynamics are taken into account. The ultimate challenge is to understand how segmental dynamics are taken into account by the central nervous system in maximizing jumping performance (5, 6).

Conclusion. I showed that the relationship between leg extension velocity and external force in leg press tasks is quasi-linear, while the relationship between leg extension velocity and muscle force is hyperbolic. The discrepancy is explained by purely mechanical factors, and there is no need to appeal to neural mechanisms to explain why, in leg press tasks, the force-velocity relationship is quasi-linear, rather than hyperbolic like Hill's relationship.

APPENDIX A: HOW LENGTH CHANGE AND FORCE OF MUSCLE-TENDON COMPLEXES RELATE TO DYNAMOMETER DISPLACEMENT AND FORCE

In this paper, only the muscle-tendon complex of *mm. vasti* was included, causing the model to be a simplified version of the original model (30) that additionally comprised the muscle-tendon complexes of *m. gluteus maximus*, hamstrings, *m. rectus femoris*, *m. soleus*, and *m. gastrocnemius* (Fig. A1). My motivation to include only one of the muscle-tendon complexes was essentially that, given the anatomical data on which the model was based (11, 32), all of these muscle-tendon complexes shorten monotonically during the leg press task, as shown in Fig. A2 (left). For the monoarticular *m. gluteus maximus*, *mm. vasti*, and *m. soleus*, this is self-evident, because the kinematic constraints of the task dictate that hip extension, knee extension, and plantar flexion occur when x_A increases. For the biarticular muscle-tendon complexes, the situation is more complicated. For hamstrings, *m. rectus femoris*, and *m. gastrocnemius*, the change in L_{MTC} (muscle-tendon complex length) depends on the ratio of the angular displacements and the ratio of the moment arms at the joints crossed. Given how the biarticular muscle-tendon complexes are embedded in the skeleton (11, 32), the net effect turns out to be that they also shorten monotonically during the leg press task (Fig. A2, left). This could actually have been predicted on the basis of the moment arm ratios of the model (30). For example, *m. rectus femoris* has an extension moment arm at the knee of 4.2 cm and a flexion moment arm at the hip of 3.5 cm. Because thighs and shanks are about equal in length, for any change in x_A , the knee angular displacement is about twice the hip angular displacement. It follows that, when the knee extends over an angular displacement $\Delta\phi$, the length change of *m. rectus femoris* amounts to $-0.042 \cdot \Delta\phi + 0.035 \cdot (0.5 \cdot \Delta\phi) = -0.0245 \cdot \Delta\phi$, which is negative (i.e., *m. rectus femoris* shortens).

When a muscle-tendon complex shortens monotonically during the leg press task, it follows that its pulling force (F_{MTC}) generates a positive (rightward directed) force component ($F_{ext-MTC}$) on the dy-

namometer. This can be explained with the principle of virtual work. Customarily, the force F_{MTC} of a muscle-tendon complex is defined as positive when it pulls on the bony insertions, and a length change δL_{MTC} is defined as positive when the complex lengthens. Now, when a muscle-tendon complex generating a force F_{MTC} changes length over a virtual distance δL_{MTC} , it produces an amount of virtual work equal to $-F_{MTC} \cdot \delta L_{MTC}$ (the minus sign solves the opposite definitions of a positive F_{MTC} and a positive δL_{MTC}). This same amount of virtual work must appear as virtual work on the dynamometer $F_{ext-MTC} \cdot \delta x_A$. If we define a transfer function (TF) as $TF = F_{ext-MTC}/F_{MTC}$, it follows that TF equals $-\delta L_{MTC}/\delta x_A$. Considering that $\delta L_{MTC}/\delta x_A$ is negative for all muscle-tendon complexes during the leg press task (Fig. A2, left), TF is positive for all muscle-tendon complexes during the leg press task (Fig. A2, right). It follows that activation of each individual muscle-tendon complexes generates a positive $F_{ext-MTC}$ on the dynamometer at all values of x_A . Hence, the outcome of the simulations will be qualitatively the same, regardless of which individual muscle-tendon complex, or combination of muscle-tendon complexes, is selected to actuate the system. The advantage of using only one muscle-tendon complex as actuator is that the results can be presented in a concise manner, and selecting the muscle-tendon complex of *mm. vasti* is a logical choice because it has the greatest value of TF at each x_A (Fig. A2, right) and also the largest force of all muscle-tendon complexes shown in Fig. A1 (30).

APPENDIX B: SYSTEM OF EQUATIONS USED FOR SIMULATIONS

To simulate the hip-knee extension task of Yamauchi et al. (35), I derived the equations of motion using a Newton Euler approach (8). Let me, for tractability in this appendix, simplify the complete system shown in Fig. 1 to the simplified two-segment (thighs and shanks) system shown in Fig. B1; the HAT segment does not play any role, since it is fixed in space, and the feet only play a minimal role because they have a small mass, which can safely be neglected. For this simplified system with no moments acting at the endpoints, we can derive the system of equations

$$A \cdot x = b \quad (B1)$$

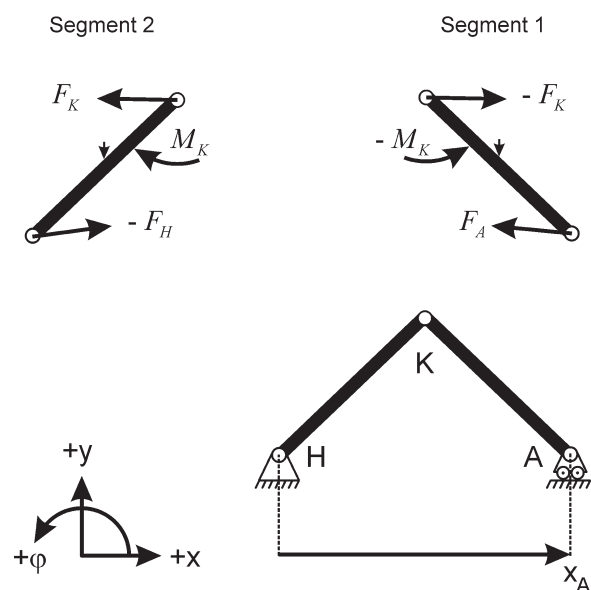


Fig. B1. Simplified model of the leg press task, and free body diagrams of the segments showing net reaction forces (F) at hips (H), knees (K), and ankles (A), as well as the joint moment at K . The forces of gravity have been plotted as small vertical arrows pointing at the segmental mass centers.

with:

$$A = \begin{bmatrix} 1 & -1 & 0 & 0 & 0 & 0 & d_1 \cdot \sin\varphi_1 \cdot m_1 & 0 & -m_1 & 0 \\ 0 & 1 & -1 & 0 & 0 & 0 & l_1 \cdot \sin\varphi_1 \cdot m_2 & d_2 \cdot \sin\varphi_2 \cdot m_2 & -m_2 & 0 \\ 0 & 0 & 0 & 1 & -1 & 0 & -d_1 \cdot \cos\varphi_1 \cdot m_1 & 0 & 0 & -m_1 \\ 0 & 0 & 0 & 0 & 1 & -1 & -l_1 \cdot \cos\varphi_1 \cdot m_2 & -d_2 \cdot \cos\varphi_2 \cdot m_2 & 0 & -m_2 \\ d_1 \cdot \sin\varphi_1 & p_1 \cdot \sin\varphi_1 & 0 & -d_1 \cdot \cos\varphi_1 & -p_1 \cdot \cos\varphi_1 & 0 & -j_1 & 0 & 0 & 0 \\ 0 & d_2 \cdot \sin\varphi_2 & p_2 \cdot \sin\varphi_2 & 0 & -d_2 \cdot \cos\varphi_2 & -p_2 \cdot \cos\varphi_2 & 0 & -j_2 & 0 & 0 \end{bmatrix}$$

$$x = \begin{bmatrix} F_A^x \\ F_K^x \\ F_H^x \\ F_A^y \\ F_K^y \\ F_H^y \\ \ddot{\varphi}_1 \\ \ddot{\varphi}_2 \\ \ddot{x}_A \\ \ddot{y}_A \end{bmatrix}$$

$$b = \begin{bmatrix} m_1 \cdot (-d_1 \cdot \cos\varphi_1 \cdot \dot{\varphi}_1^2) \\ m_2 \cdot (-l_1 \cdot \cos\varphi_1 \cdot \dot{\varphi}_1^2 - d_2 \cdot \cos\varphi_2 \cdot \dot{\varphi}_2^2) \\ m_1 \cdot (-d_1 \cdot \sin\varphi_1 \cdot \dot{\varphi}_1^2 - g) \\ m_2 \cdot (-l_1 \cdot \sin\varphi_1 \cdot \dot{\varphi}_1^2 - d_2 \cdot \sin\varphi_2 \cdot \dot{\varphi}_2^2 - g) \\ M_K \\ -M_K \end{bmatrix}$$

Here, *segment 1* represents the shanks, and *segment 2* the thighs; F^x and F^y are the net forces at the points indicated (A for ankles, K for knees, H for hips); M_K is produced by *mm. vasti* (note that knee extension moments, which are formally negative here, have been plotted positively in Figs. 2 and 3); φ_i is the angle between segment i and the right horizontal; d_i and p_i are the distances from the center of mass of segment i to the distal and proximal ends, respectively; m_i is the mass of segment i ; j_i is the moment of inertia of segment i relative to the segmental mass center; and g is the acceleration due to gravity (-9.81 m/s^2).

Horizontal and vertical acceleration of H, and vertical acceleration of A, were prevented by adding the following constraint equations:

$$\begin{bmatrix} 0 & 0 & 0 & 0 & 0 & 0 & l_1 \cdot \sin\varphi_1 & l_2 \cdot \sin\varphi_2 & -1 & 0 \\ 0 & 0 & 0 & 0 & 0 & 0 & -l_1 \cdot \cos\varphi_1 & -l_2 \cdot \cos\varphi_2 & 0 & -1 \\ 0 & 0 & 0 & 0 & 0 & 0 & 0 & 0 & 0 & 1 \end{bmatrix} \cdot x = \begin{bmatrix} -l_1 \cdot \cos\varphi_1 \cdot \dot{\varphi}_1^2 - l_2 \cdot \cos\varphi_2 \cdot \dot{\varphi}_2^2 \\ -l_1 \cdot \sin\varphi_1 \cdot \dot{\varphi}_1^2 - l_2 \cdot \sin\varphi_2 \cdot \dot{\varphi}_2^2 \\ 0 \end{bmatrix} \quad (B2)$$

In the case of isometric contractions, I also prevented horizontal acceleration of A by adding:

$$\begin{bmatrix} 0 & 0 & 0 & 0 & 0 & 0 & 0 & 0 & 1 & 0 \end{bmatrix} \cdot x = \begin{bmatrix} 0 \end{bmatrix} \quad (B3)$$

so that I had a system of 10 equations that could be solved to obtain the vector of unknowns x . In the case of dynamic contractions against an imposed external dynamometer force (F_{dyn}), I replaced Eq. B3 by:

$$\begin{bmatrix} 1 & 0 & 0 & 0 & 0 & 0 & 0 & 0 & 0 & 0 \end{bmatrix} \cdot x = \begin{bmatrix} F_{\text{dyn}} \end{bmatrix} \quad (B4)$$

Once the motion had been simulated by numerical integration, I determined the separate contributions to F_A^x in selected configurations, reached at particular time steps during the simulated motion, as follows:

1) The contribution of M_K was obtained by recalculating F_A^x in the configuration of interest using the standard set of Eq. B1, in combination with constraint Eqs. B2 and B3, but with g and all velocities and accelerations set to zero.

2) The contribution of gravity was obtained by recalculating F_A^x in the configuration of interest using the standard set of Eq. B1, in combination with constraint Eqs. B2 and B3 with M_K and all velocities and accelerations set to zero.

3) The contribution of the angular velocities was obtained by recalculating F_A^x in the configuration of interest using the standard set of Eq. B1, in combination with constraint Eqs. B2 and B3 and with the velocities at this configuration in the simulated motion, but with M_K , g , and all accelerations set to zero.

4) The contribution of the angular accelerations was obtained by recalculating F_A^x in the configuration of interest with M_K , g , and all velocities set to zero, using the standard set of Eq. B1, in combination with constraint Eq. B2 and with constraint equation

$$\begin{bmatrix} 0 & 0 & 0 & 0 & 0 & 0 & 0 & 1 & 0 & 0 \end{bmatrix} \cdot x = \begin{bmatrix} \ddot{\varphi}_{2,\text{sim}} \end{bmatrix} \quad (B5)$$

where $\ddot{\varphi}_{2,\text{sim}}$ was the angular acceleration of *segment 2* at this configuration in the simulated movement.

ACKNOWLEDGMENTS

The author thanks Knoek van Soest and Richard Casius for insightful comments on the manuscript.

DISCLOSURES

No conflicts of interest, financial or otherwise, are declared by the author.

AUTHOR CONTRIBUTIONS

M.F.B. conception and design of research; M.F.B. performed experiments; M.F.B. analyzed data; M.F.B. interpreted results of experiments; M.F.B. prepared figures; M.F.B. drafted manuscript; M.F.B. edited and revised manuscript; M.F.B. approved final version of manuscript.

REFERENCES

- Abbott BC, Wilkie DR. The relation between velocity of shortening and the tension-length curve of skeletal muscle. *J Physiol* 120: 214–223, 1953.
- Beelen A, Sargeant AJ. Effect of fatigue on maximal power output at different contraction velocities in humans. *J Appl Physiol* 71: 2332–2337, 1991.

3. Bobbert MF, Casius LJ, Sijpkens IW, Jaspers RT. Humans adjust control to initial squat depth in vertical squat jumping. *J Appl Physiol* 105: 1428–1440, 2008.
4. Bobbert MF, Harlaar J. Evaluation of moment-angle curves in isokinetic knee extension. *Med Sci Sports Exerc* 25: 251–259, 1993.
5. Bobbert MF, van Ingen Schenau GJ. Coordination in vertical jumping. *J Biomech* 21: 249–262, 1988.
6. Bobbert MF, van Soest AJ. Why do people jump the way they do? *Exerc Sport Sci Rev* 29: 95–102, 2001.
7. Bosco C, Belli A, Astrua M, Tihanyi J, Pozzo R, Kellis S, Tsarpela O, Foti C, Manno R, Tranquilli C. A dynamometer for evaluation of dynamic muscle work. *Eur J Appl Physiol Occup Physiol* 70: 379–386, 1995.
8. Casius LJR, Bobbert MF, van Soest AJ. Forward dynamics of two-dimensional skeletal models. A Newton-Euler approach. *J Appl Biomech* 20: 421–449, 2004.
9. Ebashi S, Endo M. Calcium ion and muscle contraction. *Prog Biophys Mol Biol* 18: 123–183, 1968.
10. Fenn WO, Marsh BS. Muscular force at different speeds of shortening. *J Physiol* 85: 277–297, 1935.
11. Grieve DW, Pheasant S, Cavanagh PR. Prediction of gastrocnemius length from knee and ankle joint posture. In: *Biomechanics VI-A*, edited by Asmussen E and Jorgensen K. Baltimore, MD: University Park Press, 1978, p. 405–412.
12. Hatze H. A myocybernetic control model of skeletal muscle. *Biol Cybern* 25: 103–119, 1977.
13. Hill AV. The heat of shortening and the dynamic constants of muscle. *Proc R Soc Lond B Biol Sci* 126: 136–159, 1938.
14. Hintzy F, Tordi N, Predine E, Rouillon JD, Belli A. Force-velocity characteristics of upper limb extension during maximal wheelchair sprinting performed by healthy able-bodied females. *J Sports Sci* 21: 921–926, 2003.
15. Huxley AF. Muscle structure and theories of contraction. *Prog Biophys Biophys Chem* 7: 255–318, 1957.
16. Lenaerts A, Verbruggen LA, Duquet W. Reproducibility and reliability of measurements using a linear isokinetic dynamometer, Aristokin. *J Sports Med Phys Fitness* 41: 362–370, 2001.
17. Macaluso A, De Vito G. Comparison between young and older women in explosive power output and its determinants during a single leg-press action after optimisation of load. *Eur J Appl Physiol* 90: 458–463, 2003.
18. Pearson SJ, Cobbold M, Harridge SD. Power output of the lower limb during variable inertial loading: a comparison between methods using single and repeated contractions. *Eur J Appl Physiol* 92: 176–181, 2004.
19. Perrine JJ, Edgerton VR. Muscle force-velocity and power-velocity relationships under isokinetic loading. *Med Sci Sports* 10: 159–166, 1978.
20. Rahmani A, Viale F, Dalleau G, Lacour JR. Force/velocity and power/velocity relationships in squat exercise. *Eur J Appl Physiol* 84: 227–232, 2001.
21. Ralston HJ, Inman VT, Strait LA, Shaffrath MD. Mechanics of human isolated voluntary muscle. *Am J Physiol* 151: 612–620, 1947.
22. Rejc E, Lazzar S, Antonutto G, Isola M, di Prampero PE. Bilateral deficit and EMG activity during explosive lower limb contractions against different overloads. *Eur J Appl Physiol* 108: 157–165, 2010.
23. Samozino P, Morin JB, Hintzy F, Belli A. Jumping ability: a theoretical integrative approach. *J Theor Biol* 264: 11–18, 2010.
24. Sargeant AJ, Hoinville E, Young A. Maximum leg force and power output during short-term dynamic exercise. *J Appl Physiol* 51: 1175–1182, 1981.
25. Shampine LF, Gordon MK. *Computer Solution of Ordinary Differential Equations. The Initial Value Problem*. San Francisco, CA: Freeman, 1975.
26. van Ingen Schenau GJ. From rotation to translation—constraints on multi-joint movements and the unique action of bi-articular muscles. *Hum Mov Sci* 8: 301–337, 1989.
27. van Ingen Schenau GJ, Cavanagh PR. Power equations in endurance sports. *J Biomech* 23: 865–881, 1990.
28. van Soest AJ, Bobbert MF. The contribution of muscle properties in the control of explosive movements. *Biol Cybern* 69: 195–204, 1993.
29. van Soest AJ, Casius LJ. Which factors determine the optimal pedaling rate in sprint cycling? *Med Sci Sports Exerc* 32: 1927–1934, 2000.
30. van Soest AJ, Schwab AL, Bobbert MF, van Ingen Schenau GJ. The influence of the biarticularity of the gastrocnemius muscle on vertical-jumping achievement. *J Biomech* 26: 1–8, 1993.
31. Vandewalle H, Peres G, Heller J, Panel J, Monod H. Force-velocity relationship and maximal power on a cycle ergometer. Correlation with the height of a vertical jump. *Eur J Appl Physiol Occup Physiol* 56: 650–656, 1987.
32. Visser JJ, Hoogkamer JE, Bobbert MF, Huijing PA. Length and moment arm of human leg muscles as a function of knee and hip-joint angles. *Eur J Appl Physiol Occup Physiol* 61: 453–460, 1990.
33. Wickiewicz TL, Roy RR, Powell PL, Perrine JJ, Edgerton VR. Muscle architecture and force-velocity relationships in humans. *J Appl Physiol* 57: 435–443, 1984.
34. Wilkie DR. The relation between force and velocity in human muscle. *J Physiol* 110: 249–280, 1949.
35. Yamauchi J, Mishima C, Fujiwara M, Nakayama S, Ishii N. Steady-state force-velocity relation in human multi-joint movement determined with force clamp analysis. *J Biomech* 40: 1433–1442, 2007.
36. Yamauchi J, Mishima C, Nakayama S, Ishii N. Aging-related differences in maximum force, unloaded velocity and power of human leg multi-joint movement. *Gerontology* 56: 167–174, 2010.
37. Yamauchi J, Mishima C, Nakayama S, Ishii N. Force-velocity, force-power relationships of bilateral and unilateral leg multi-joint movements in young and elderly women. *J Biomech* 42: 2151–2157, 2009.